

New Synthetic Routes to a Disulfidodinickel(II) Complex: Characterization and Reactivity of a $\text{Ni}_2(\mu\text{-}\eta^2\text{:}\eta^2\text{-S}_2)$ Core

Jaeheung Cho,^{†,‡} Katherine M. Van Heuvelen,[§] Glenn P. A. Yap,[†] Thomas C. Brunold,[§] and Charles G. Riordan^{*,†}

Department of Chemistry and Biochemistry, University of Delaware, Newark, Delaware 19716, and Department of Chemistry, University of Wisconsin—Madison, Madison, Wisconsin 53706

Received February 21, 2008

Activation of elemental sulfur by the monovalent nickel complex $[\text{PhTi}^{\text{tBu}}\text{Ni}(\text{CO})]$ [PhTi^{tBu} = phenyl{tris[(*tert*-butylmethyl)thio]methyl}borate] generates the disulfidodinickel(II) complex **2**. This species is alternatively accessible via thermal decomposition of $[\text{PhTi}^{\text{tBu}}\text{Ni}(\text{SCPh}_3)]$. Spectroscopic, magnetic, and X-ray diffraction studies establish that **2** contains a $\mu\text{-}\eta^2\text{:}\eta^2\text{-S}_2$ ligand that fosters antiferromagnetic exchange coupling between the Ni^{II} ions. This observation is in contrast to the lighter congener, oxygen, which strongly favors the bis($\mu\text{-oxo}$)dinickel(III) structure. **2** oxidizes PPh_3 to SPPH_3 and reacts with O_2 , generating several products, one of which has been identified as $[(\text{PhTi}^{\text{tBu}}\text{Ni})_2(\mu\text{-S})]$ (**3**).

The activation of O_2 by monovalent nickel complexes has proven to be a productive approach to the generation of new, metastable Ni_xO_y species that include side-on and end-on superoxo and *trans*- $\mu\text{-1,2}$ -peroxo motifs.¹ Initial investigations focused primarily on exploring the geometric and electronic structures of these compounds, characteristics that are fundamental in understanding their stability and reactivity. Recently, we have turned our attention to the heavier congener sulfur, with the expectation that a similarly diverse range of structures may be kinetically accessible via the analogous synthetic route, i.e., reaction of a nickel(I) precursor with elemental sulfur. These new structure types are anticipated to display novel magnetic properties and reactivity. For example, nickel sulfides are effective catalysts for hydrogenation² and hydrodesulfurization³ and have been explored as cathode materials for rechargeable lithium batteries.⁴ Previous reports of soluble nickel sulfide complexes include sulfido-^{5,6} and disulfido-bridged^{7–9} species in which the bridges are most commonly derived from hydrogen sulfide (or its conjugate bases) via acid–base reactions.

Alternative preparative routes include atom transfer from cyclohexene sulfide and 1,2-elimination from $(\text{dcpe})\text{Ni}(\text{SH})\text{Ph}$, generating an inferred terminal sulfide, $(\text{dcpe})\text{NiS}$, that dimerizes to a di- $\mu\text{-sulfido}$ complex.³ Two of the $\text{Ni}_2(\mu\text{-}\eta^2\text{:}\eta^2\text{-S}_2)$ complexes have been structurally characterized, a dinickel(II) species with N donors⁷ and the mixed-valent, nickel(II)–nickel(I) complex ligated by a triphosphine ligand.⁸ However, neither the reactivity nor the full magnetic properties¹⁰ of these complexes have been reported. Also, we are unaware of reports detailing the synthesis of nickel sulfide complexes via the reaction of nickel(I) and sulfur. Analogous copper sulfide chemistry has seen a renaissance with the identification of the $\text{Cu}_4(\mu^4\text{-S})$ (Cu_2) cluster in the enzyme nitrous oxide reductase.¹¹ For example, Karlin and co-workers reported the synthesis of $\text{Cu}_2(\mu\text{-1,2-S}_2)$ ¹² and $\text{Cu}_2(\mu\text{-}\eta^2\text{:}\eta^2\text{-S}_2)$ ¹³ complexes as well as their reactivity with exogenous substrates. Tolman's laboratory has highlighted ligand structural effects on the $\text{Cu}_2(\mu\text{-}\eta^2\text{:}\eta^2\text{-S}_2)$ core bonding^{14,15} as well as prepared higher nuclearity species contain-

* To whom correspondence should be addressed. E-mail: riordan@udel.edu.

[†] University of Delaware.

[‡] Current address: Department of Chemistry and Nano Science, Center for Biomimetic Systems, Ewha Womans University, Seoul 120-750, Korea.

[§] University of Wisconsin—Madison.

- (1) Kieber-Emmons, M. T.; Riordan, C. G. *Acc. Chem. Res.* **2007**, *40*, 618.
- (2) Olivas, A.; Cruz-Reyes, J.; Petranovskii, V.; Avalos, M.; Fuentes, S. *J. Vac. Sci. Technol., A* **1998**, *16*, 3515.
- (3) Vivic, D. A.; Jones, W. D. *J. Am. Chem. Soc.* **1999**, *121*, 7606.

- (4) Han, S. C.; Kim, H. S.; Song, M. S.; Kim, J. H.; Ahn, H. J.; Lee, J. Y. *J. Alloys Compd.* **2003**, *351*, 273.
- (5) (a) Kruger, T.; Krebs, B.; Henkel, G. *Angew. Chem., Int. Ed. Engl.* **1989**, *28*, 61. (b) Oster, S. S.; Lachicotte, R. J.; Jones, W. D. *Inorg. Chim. Acta* **2002**, *330*, 118.
- (6) Mealli, C.; Midollini, S.; Sacconi, L. *Inorg. Chem.* **1978**, *17*, 632.
- (7) Pleus, R. J.; Waden, H.; Saak, W.; Haase, D.; Pohl, S. *J. Chem. Soc., Dalton Trans.* **1999**, 2601.
- (8) Mealli, C.; Midollini, S. *Inorg. Chem.* **1983**, *22*, 2785.
- (9) Tremel, W.; Henkel, G. *Inorg. Chem.* **1988**, *27*, 3896.
- (10) The bulk magnetic moment and 77 K EPR spectrum of the mixed-valence complex were reported.
- (11) Chen, P.; Gorelsky, S. I.; Ghosh, S.; Solomon, E. I. *Angew. Chem.* **2004**, *116*, 4224.
- (12) (a) Maiti, D.; Woertink, J. S.; Vance, M. A.; Milligan, A. E.; Sarjeant, A. N. N.; Solomon, E. I.; Karlin, K. D. *J. Am. Chem. Soc.* **2007**, *129*, 8882. (b) Helton, M. E.; Chen, P.; Paul, P. P.; Tyeklar, Z.; Sommer, R. D.; Zakharov, L. N.; Rheingold, A. L.; Solomon, E. I.; Karlin, K. D. *J. Am. Chem. Soc.* **2003**, *125*, 1160.
- (13) Helton, M. E.; Maiti, D.; Zakharov, L. N.; Rheingold, A. L.; Porco, J. A.; Karlin, K. D. *Angew. Chem., Int. Ed.* **2006**, *45*, 1138.
- (14) Brown, E. C.; Bar-Nahum, I.; York, J. T.; Aboeella, N. W.; Tolman, W. B. *Inorg. Chem.* **2007**, *46*, 486.
- (15) Brown, E. C.; Aboeella, N. W.; Reynolds, A. M.; Aullon, G.; Alvarez, S.; Tolman, W. B. *Inorg. Chem.* **2004**, *43*, 3335.

Scheme 1

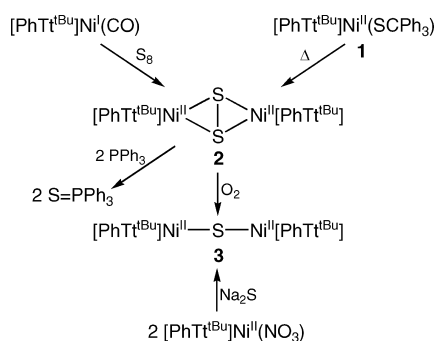


Figure 1. Structure of **2**. Thermal ellipsoids are at the 50% level, and H atoms are omitted. Selected bond lengths (Å) and angles (deg): S4–S4* 2.177(2), Ni–S1 2.304(1), Ni–S2 2.315(1), Ni–S3 2.311(1), Ni–S4 2.242(1), Ni–S4* 2.248(1), Ni⋯Ni* 3.926; Ni–S4–Ni* 121.99(4), S4–Ni–S4* 58.01(4).

ing $[\text{Cu}_3(\mu\text{-S})_2]^{3+}$,¹⁶ $[\text{Cu}_4(\mu\text{-S}_2)_2]^{4+}$, and/or $[\text{Cu}_6(\mu\text{-S}_2)_4]^{4+}$ cores.¹⁷ Detailed electronic structure descriptions for several of these complexes have very recently been presented.¹⁸

Herein, we report the structural and spectroscopic characterization of a $\mu\text{-}\eta^2\text{:}\eta^2\text{-disulfido}$ nickel(II) complex, $[(\text{PhTt}^{\text{tBu}})\text{Ni}]_2(\mu\text{-}\eta^2\text{:}\eta^2\text{-S}_2)$ (**2**), prepared by following either of two synthetic routes: (i) reaction of S_8 with the nickel(I) complex $[\text{PhTt}^{\text{tBu}}]\text{Ni}(\text{CO})$ ¹⁹ or (ii) the thermal decomposition of the nickel(II) complex $[\text{PhTt}^{\text{tBu}}]\text{Ni}(\text{SCPh}_3)$ (**1**) via C–S bond cleavage (Scheme 1). The latter route is inspired by the seminal study of Kitajima and Fujisawa²¹ in which trityl thiolate decomposition was shown to be an effective preparative strategy for the synthesis of a Cu_2S_2 core.²² The structural and spectroscopic characterizations of **2**, and its reactivity with PPh_3 and O_2 , the latter leading to a μ -sulfido nickel complex, are detailed.

Stirring a solution of **1** under N_2 at room temperature for several hours afforded a color change from dark violet to dark brown, signifying the formation of **2** via C–S bond rupture (Scheme 1).²¹ This complex is also accessible from the reaction of $[\text{PhTt}^{\text{tBu}}]\text{Ni}(\text{CO})$ with S_8 , although this reaction requires 1 week to reach completion. In contrast to the latter reaction, the reactions of copper(I) precursors with S_8 and the oxygenation of $[\text{PhTt}^{\text{tBu}}]\text{Ni}(\text{CO})$ proceed within minutes to hours. The optical spectra of samples of **2** prepared by either route are indistinguishable. An X-ray diffraction study revealed that **2** consists of a centrosymmetric $\text{Ni}_2(\mu\text{-}\eta^2\text{:}\eta^2\text{-S}_2)$ core in a slightly distorted square-pyramidal geometry ($\tau = 0.1$),²³ as shown in Figure 1. The S–S bond distance, 2.177(2) Å, is shorter than that found in $\{[(\text{cyclam})\text{Ni}]_2(\mu\text{-}\eta^2\text{:}\eta^2\text{-S}_2)\}^{2+}$ [2.297(4) Å]⁷ and $\{[(\text{triphos})\text{Ni}]_2(\mu\text{-}\eta^2\text{:}\eta^2\text{-S}_2)\}^+$ [2.208(4) Å].⁸ The elongated S–S distances found in the latter two species point to even more reduced (S_2)²⁻ linkages resulting from greater back-donation

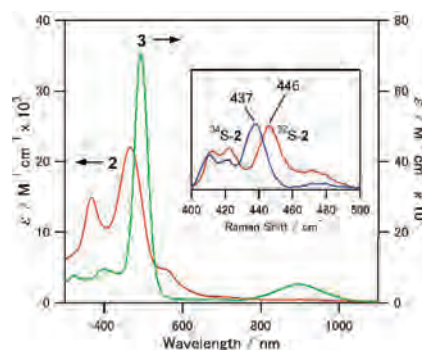


Figure 2. Electronic spectra of **2** (red line) and **3** (green line) in chloroform at room temperature. The inset shows the rR spectra ($\lambda_{\text{ex}} = 472 \text{ nm}$) of frozen chloroform solutions (77 K) of **2** (red line for ^{32}S -**2**; blue line for ^{34}S -**2**).

from the electron-rich metal to the $\text{S}_2 \sigma^*$ orbital. Population of this S_2 antibonding orbital serves to weaken and lengthen the S–S bond. This increased electron density derives, in large part, from the higher coordination number provided by cyclam in $\{[(\text{cyclam})\text{Ni}]_2(\mu\text{-}\eta^2\text{:}\eta^2\text{-S}_2)\}^{2+}$ and the $\text{Ni}^{\text{II}}\text{Ni}^{\text{I}}$ valency in $\{[(\text{triphos})\text{Ni}]_2(\mu\text{-}\eta^2\text{:}\eta^2\text{-S}_2)\}^+$.

The optical spectrum of **2** displays an intense band centered at $\lambda_{\text{max}} = 466 \text{ nm}$ ($\epsilon = 22\,000 \text{ M}^{-1} \text{cm}^{-1}$) and a shoulder at $\sim 560 \text{ nm}$ ($\epsilon = 4700 \text{ M}^{-1} \text{cm}^{-1}$) (Figure 2), which are tentatively assigned as the disulfide $\pi^*_{\sigma} \rightarrow \text{Ni}^{\text{II}}$ and $\pi^*_{\nu} \rightarrow \text{Ni}^{\text{II}} d_{x^2-y^2}$ charge-transfer (CT) transitions, respectively, from comparison with the absorption spectra of analogous $\text{Cu}_2(\mu\text{-}\eta^2\text{:}\eta^2\text{-S}_2)$ complexes.²² The resonance Raman (rR) spectrum ($\lambda_{\text{ex}} = 472 \text{ nm}$; $T = 77 \text{ K}$) of **2** in chloroform exhibits an isotopically sensitive band at 446 cm^{-1} [$\Delta(^{32}\text{S}-^{34}\text{S}) = 9 \text{ cm}^{-1}$; Figure 2 (inset)]. On the basis of its isotope shift and the fact that it is strongly resonance-enhanced for excitation into the dominant disulfide $\pi^*_{\sigma} \rightarrow \text{Ni}^{\text{II}}$ absorption band at 466 nm , this feature is assigned to the S–S stretching mode of the $\text{Ni}_2(\mu\text{-}\eta^2\text{:}\eta^2\text{-S}_2)$ core. The energy of this band is within the range of the $\nu_{\text{S-S}}$ values reported for other transition-metal disulfido complexes ($424\text{--}613 \text{ cm}^{-1}$).¹⁴ The observed isotopic shift is smaller than that predicted for a diatomic harmonic oscillator ($\sim 13 \text{ cm}^{-1}$), which may be attributed to mixing between the S–S and Ni–S stretching motions. The relatively low $\nu_{\text{S-S}}$ frequency is consistent with the larger S–S bond distance in **2** than in most previously characterized disulfido metal complexes. Indeed, these data are correlated via the empirical relationship known as Badger's rule, which has recently been applied by Tolman to disulfido metal complexes.¹⁴ The low

- (16) Brown, E. C.; York, J. T.; Antholine, W. E.; Ruiz, E.; Alvarez, S.; Tolman, W. B. *J. Am. Chem. Soc.* **2005**, *127*, 13752.
 (17) York, J. T.; Bar-Nahum, I.; Tolman, W. B. *Inorg. Chem.* **2007**, *46*, 8105.
 (18) Sarangi, R.; York, J. T.; Helton, M. E.; Fujisawa, K.; Karlin, K. D.; Tolman, W. B.; Hodgson, K. O.; Hedman, B.; Solomon, E. I. *J. Am. Chem. Soc.* **2008**, *130*, 676.
 (19) Schebler, P. J.; Mandimutsira, B. S.; Riordan, C. G.; Liable-Sands, L.; Incarvito, C. D.; Rheingold, A. L. *J. Am. Chem. Soc.* **2001**, *123*, 331.
 (20) Cho, J.; Yap, G. P. A.; Riordan, C. G. *Inorg. Chem.* **2007**, *46*, 11308.
 (21) Fujisawa, K.; Moro-oka, Y.; Kitajima, N. *J. Chem. Soc., Chem. Commun.* **1994**, 623. This complex was subsequently prepared by the reaction of copper(I) and S_8 .²²
 (22) Chen, P.; Fujisawa, K.; Helton, M. E.; Karlin, K. D.; Solomon, E. I. *J. Am. Chem. Soc.* **2003**, *125*, 6394.
 (23) Addison, A. W.; Rao, T. N.; Reedijk, J.; Vanrijn, J.; Verschoor, G. C. *J. Chem. Soc., Dalton Trans.* **1984**, 1349.

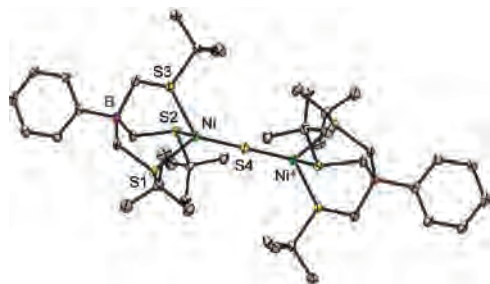


Figure 3. Structure of **3**. Thermal ellipsoids are at the 50% level, and H atoms are omitted. Selected bond lengths (Å) and angles (deg): Ni–S1 2.2869(6), Ni–S2 2.2948(7), Ni–S3 2.2839(6), Ni–S4 2.0714(4), Ni···Ni* 4.143; Ni–S4–Ni* 180.

ν_{S-S} value and long S–S distance place **2** near one end of this correlation, lending support for the $(S_2)^{2-}$ formalism.

Complex **2** is electron paramagnetic resonance (EPR) silent at 77 K and exhibits a well-resolved ^1H NMR spectrum in the $\delta = 0\text{--}10$ region at room temperature (see the Supporting Information). The resonances for the *tert*-butyl and phenyl protons were observed at $\delta = 1.68$ and in the $\delta = 7.51\text{--}7.12$ range, respectively. These observations suggest that **2** possesses a diamagnetic ground state. However, a relatively broad ($\Delta\nu_{1/2} = 54$ Hz) peak at $\delta = 7.67$ assigned to the methylene protons displays an upfield shift with decreasing temperature, characteristic of anti-Curie behavior. A similar temperature dependence was also noted for the *tert*-butyl resonances, indicating that **2** is composed of two high-spin ($S = 1$) Ni^{II} ions that are antiferromagnetically coupled to yield an $S = 0$ ground state. From a quantitative analysis of the temperature dependence of the NMR spectral data, we estimate that $J = -476(3) \text{ cm}^{-1}$ ($H = -2JS_1 \cdot S_2$).²⁴ Similarly, large exchange coupling constants have been estimated for $\mu\text{-}\eta^2\text{:}\eta^2\text{-disulfidodicopper(II)}$ complexes, i.e., $|2J| \geq 600 \text{ cm}^{-1}$.^{15,21}

Complex **2** reacts under aerobic conditions to generate the diamagnetic species $[(\text{PhTt}^{\text{tBu}}\text{Ni})_2(\mu\text{-S})]$ (**3**) in low crystalline yield (6%).²⁵ As in the case of **2**, **3** can be accessed by two distinct synthetic pathways; the independent reaction of $[\text{PhTt}^{\text{tBu}}\text{Ni}(\text{NO}_3)]$ with Na_2S yields a product that is spectroscopically indistinguishable from that obtained by exposing **2** to air. The X-ray structure of **3** revealed that the two nickel centers are bridged by a single sulfido ligand and adopt a distorted tetrahedral geometry ($\tau = 0.27$)²⁶ (Figure 3). The Ni–S4 bond distance of 2.0714(4) Å and Ni–S–Ni angle of 180° are comparable to the analogous structural parameters reported for $\{[(\text{p}_3)\text{Ni}]_2(\mu\text{-S})\}^{2+}$ [$\text{p}_3 = \text{CH}_3\text{C}(\text{CH}_2\text{PPh}_2)_3$] of 2.034 Å and 180° , respectively.⁶ The Ni–S bond distance in **3** [2.0714(4) Å] is significantly shorter than those in **2** [2.242(1) and 2.248(1) Å], while the opening of the Ni–S–Ni angle (from 121.99° to 180°) gives rise to an

elongation of the Ni···Ni distance (from 3.926 to 4.143 Å). **3** was characterized by electronic absorption and ^1H NMR spectroscopies. A very intense optical band centered at $\lambda_{\text{max}} = 494 \text{ nm}$ ($\epsilon = 70\,000 \text{ M}^{-1} \text{ cm}^{-1}$) is tentatively assigned as a $\mu\text{-sulfido} \rightarrow \text{Ni}^{\text{II}}$ CT transition (Figure 2). **3** was found to possess a diamagnetic ground state at room temperature, as evidenced by its ^1H NMR spectrum and the lack of a magnetic moment. Collectively, these results suggest that **3** is composed of two antiferromagnetically coupled high-spin ($S = 1$) Ni^{II} ions, similar to **2**.

Interestingly, the reactivity of **2** with O_2 is quite different from that reported for its copper analogues. In particular, the $\text{Cu}_2(\mu\text{-}\eta^2\text{:}\eta^2\text{-S}_2)$ complex prepared by Karlin's group, which possesses a neutral tridentate N-donor ligand, reacts with O_2 to yield a $\mu\text{-}\eta^2\text{:}\eta^2\text{-peroxocopper(II)}$ species at low temperature,¹³ whereas **2** does not react with O_2 at low temperatures, conditions under which the bis($\mu\text{-oxo}$)dinickel(III) complex persists.²⁷ Alternatively, Tolman's $\text{Cu}_2(\mu\text{-}\eta^2\text{:}\eta^2\text{-S}_2)$ complexes that are supported by anionic bidentate N-donor ligands do not react with O_2 .¹⁴ Although the details concerning the oxygenation of **2** including the establishment of the major product(s) remain to be established, additional reactivity studies were carried out to obtain insight into the character of the $\text{Ni}_2(\mu\text{-}\eta^2\text{:}\eta^2\text{-S}_2)$ core in **2** (Scheme 1). The reaction of **2** with 2 equiv of PPh_3 generates $\text{S}=\text{PPh}_3$ quantitatively (see the Supporting Information for details). Thus, the electrophilic character of **2** is similar to that reported recently for copper analogues.^{13,14}

In summary, complex **2** is accessible via two independent and complementary synthetic routes, namely, the activation of elemental sulfur by nickel(I) and the thermal decomposition of **1** via C–S bond cleavage. This report establishes the reaction of nickel(I) with elemental sulfur as a new synthetic strategy for the preparation of sulfidonicel adducts. In contrast to oxygenation, which leads to the thermally unstable dinickel(III) complex $[(\text{PhTt}^{\text{tBu}}\text{Ni})_2(\mu\text{-O})_2]$, **2** contains a distinctly stable dichalcogenide core. As such, **2** serves as a model for hitherto unobserved $\mu\text{-}\eta^2\text{:}\eta^2\text{-peroxodinickel}$ complexes. Exposure of **2** to O_2 yields the $\text{Ni}_2(\mu\text{-S})$ complex **3**, albeit in low yield. Efforts to identify the major product(s) of this reaction remain ongoing. The reactivity of **2** toward O_2 is distinct from that reported for analogous copper complexes. Further elucidation of the magnetic properties, electronic structures, and reactivities of **2** and **3** is underway.

Acknowledgment is made to the NSF (Grant CHE-0518508) by C.G.R. and to the NSF Graduate Research Fellowship Program by K.M.V.H. We thank Matt Kieber-Emmons for fitting the variable-temperature ^1H NMR data.

Supporting Information Available: Synthetic procedures and characterization data (PDF) and X-ray diffraction refinement data for **2** and **3** (CIF). This material is available free of charge via the Internet at <http://pubs.acs.org>.

IC800321X

(24) The ^1H NMR spectral data were recorded between 213 and 313 K and fitted to the effective Hamiltonian as detailed in the Supporting Information.

(25) The reaction of **2** with O_2 produces at least two products; the minor species is **3**. The major species (>80%), as deduced by ^1H NMR spectroscopy, displays paramagnetically shifted resonances typical for a $[\text{PhTt}^{\text{tBu}}\text{Ni}]^{\text{II}}$ species. Efforts to identify this product continue.

(26) Vela, J.; Stoian, S.; Flaschenriem, C. J.; Münck, E.; Holland, P. L. *J. Am. Chem. Soc.* **2004**, *126*, 4522.

(27) Mandimutsira, B. S.; Yamarik, J. L.; Brunold, T. C.; Gu, W.; Cramer, S. P.; Riordan, C. G. *J. Am. Chem. Soc.* **2001**, *123*, 9194.